

3D Elastostatic Boundary Element Analysis of Ultra-Thin Structures with Planar Surfaces

*Y.C. Shiah¹, Y.M. Lee², and R.B. Yang²

¹ Department of Aeronautics and Astronautics
National Cheng Kung University, Tainan 701, Taiwan.

² Department of Aerospace and Systems Engineering,
Feng Chia University, Taichung 40724, Taiwan

*Corresponding author: ycshiah@mail.ncku.edu.tw

Abstract

This paper presents a regularization scheme for the nearly singular integrals used for 3D elastostatic boundary element analysis. For the regularization process, the local projection coordinates of the source point are first located via an iteration procedure. For planar elements, the boundary integrals are analytically integrated by parts to smooth the drastic fluctuations of their integrands so that the regularized forms can be numerically integrated by any conventional schemes in an usual manner. The validity of the formulations is numerically tested using the Gauss Quadrature scheme. The test shows the accuracy is satisfactory for the distance ratio (distance : element characteristic length) falling below micro-scale.

Keywords: Boundary integral regularization, 3D elastostatic BEM analysis

Introduction

In these years, the boundary element method, usually abbreviated as BEM, has been widely applied to various engineering problems due to its distinctive feature that only the boundary needs discretisation. In particular, this is most advantageous in modeling three-dimensional problems with complicated geometry that demands heavy modeling efforts for the domain solution techniques, such as the finite element method (FEM) and the finite difference method. In engineering applications, ultra-thin structures are quite often applied that are characterized by their thickness dimensioned with several orders below their characteristic length. For yielding reliable results by the FEM analysis, the elements employed must have proper aspect ratios that are normally greater than 1:20. Due to this aspect-ratio constraint, the FEM-modeling of ultra-thin structures shall take tremendous amounts of elements, leading to overloading computations. Although no such issue is involved for the BEM, another difficulty of “near singularity” will arise. As has been well understood in the BEM community, approaching of the source point to the element under integration will lead to drastic fluctuation of the integrands near its projection place and cause difficulty of proper numerical integration.

Over the years, this topic of nearly singular integrals has attracted significant researches in the BEM community. The most known approaches for dealing with this issue can be referred to (e.g. Zozulya, 2010; Chen and Hong, 1999; Guz and Zozulya, 2001; Tanaka et al., 1994). For the BEM analysis, ultra-thin structures with flat or less-curved surfaces can be modeled by assemblage of planar elements. In this subcategory of planar elements, the main goal of the present work targets regularizing the boundary integrals for the BEM elastostatic analysis by an approach of “integration by parts”, abbreviated as IBP in this paper. There are too many articles to review as a complete for the topic of integral regularizations; only a few among them are mentioned herein as examples. Granados and Gallego (2001) proposed a kernels' complex regularization procedure, leading to a decomposition of the quasi-singular and quasi-hypersingular integrals in a series of simpler terms. Recently, Tomioka and Nishiyama (2010) presented a gradient field representation using an analytical regularization of a hypersingular boundary integral equation for the Helmholtz equation. For axisymmetric linear elasticity, de Lacerda and Wrobel (2001) presented a hypersingular boundary integral equation, which are regularized by employing the singularity subtraction technique. On applying the IBP, Shiah and Shi (2006) regularized the boundary integrals for the 2D anisotropic heat conduction problems. Furthermore, Shiah *et al.* (2007) applied this IBP technique to study the 2D interlaminar thermal stresses in thin layers of composites. To the authors' best

knowledge, no implementation of the IBP in 3D elastostatic BEM analysis has been reported in the open literature yet. The present work is to extend the IBP work (2006) for 2D cases to treat the boundary integrals of the 3D elastostatics for ultra-thin bodies with planar surfaces. For numerical tests, the regularized integrals of a typical case were evaluated using the conventional 14-point Gauss quadrature scheme and compared with the numerical results obtained by mathematical software. Before presenting the regularization scheme, a brief review of the boundary integral equation for 3D elastostatic analysis will be given next

Boundary integral equation of 3D Elastostatics

In the direct formulation of BEM, the displacements u_i and the tractions t_i at the source point P and the field point Q on the surface S of an elastic body are related by the following integral equation,

$$C_{ij}(P) u_i(P) = \int_S t_i(Q) U_{ij}^*(P, Q) dS - \int_S u_i(Q) T_{ij}^*(P, Q) dS, \quad (1)$$

where C_{ij} are geometrically dependent coefficients at P , q is an arbitrary field point inside the domain V ; U_{ij}^* and T_{ij}^* are respectively the fundamental solutions of the displacements and tractions, given for 2D isotropic elastic bodies by

$$U_{ij}^*(P, Q) = \frac{1}{16\pi G(1-\nu)r} \left[(3-4\nu)\delta_{ij} + r_i r_{,j} \right], \quad (2a)$$

$$T_{ij}^*(P, Q) = \frac{-1}{8\pi(1-\nu)r^2} \left\{ r_{,k} n_k \left[(1-2\nu)\delta_{ij} + 3r_i r_{,j} \right] - (1-2\nu)(r_i n_j - r_{,j} n_i) \right\}, \quad (2b)$$

where ν stands for the Poisson's ratio, G is the shear modulus, δ_{ij} stands for the Kronecker delta defined as usual, n_i are the components of the outward normal vector, and r represents the radial distance between the source point at (x_1, x_2, x_3) and the field point at (xp_1, xp_2, xp_3) and $r_{,i}$ represents taking partial differentiation of r with respect to x_i . They are calculated by

$$r = \sqrt{\sum_{l=1}^3 (x_l - xp_l)^2}, \quad r_{,i} = \frac{(x_i - xp_i)}{\sqrt{\sum_{l=1}^3 (x_l - xp_l)^2}}. \quad (3)$$

Apparently, when the source point approaches the field point i.e. $r \approx 0$, Eq.(2a) and (2b) reveal singularities with orders $O(1/r)$ and $O(1/r^2)$, respectively. As the usual BEM process for solving Eq.(1), the boundary is discretized into a number of elements, say M elements, with k nodes on each one. As a result of interpolating the nodal values of $u_i^{(c)}$, $t_i^{(c)}$ by the shape functions $N^{(c)}(\xi, \eta)$, the displacements/tractions at Q can be written as

$$u_i(Q) = \sum_{c=1}^k N^{(c)}(\xi, \eta) u_i^{(c)}, \quad t_i(Q) = \sum_{c=1}^k N^{(c)}(\xi, \eta) t_i^{(c)}, \quad (4)$$

where (ξ, η) are the intrinsic local coordinates on each integration element. For an assemblage of M -elements, substitution of Eq.(4) into Eq.(1) yields a discretized integral equation as follows,

$$C_{ij}(P) u_i(P) = \sum_{m=1}^M \sum_{c=1}^k t_{i(m)}^{(c)} \int_{-1}^1 \int_{-1}^1 N^{(c)}(\xi, \eta) U_{ij}^* |J(\xi, \eta)| d\xi d\eta - \sum_{m=1}^M \sum_{c=1}^k u_{i(m)}^{(c)} \int_{-1}^1 \int_{-1}^1 N^{(c)}(\xi, \eta) T_{ij}^* |J(\xi, \eta)| d\xi d\eta, \quad (5)$$

where the subscript (m) is used to denote the m -th discretized element, and $|J(\xi, \eta)|$ is the Jacobian transformation, defined by

$$|J(\xi, \eta)| = \sqrt{J_1^2 + J_2^2 + J_3^2}, \quad (6a)$$

$$J_1 = \left(\sum_{c=1}^k N_{,\xi}^{(c)} x_2^{(c)} \right) \left(\sum_{c=1}^k N_{,\eta}^{(c)} x_3^{(c)} \right) - \left(\sum_{c=1}^k N_{,\xi}^{(c)} x_3^{(c)} \right) \left(\sum_{c=1}^k N_{,\eta}^{(c)} x_2^{(c)} \right), \quad (6b)$$

$$J_2 = \left(\sum_{c=1}^k N_{,\xi}^{(c)} x_3^{(c)} \right) \left(\sum_{c=1}^k N_{,\eta}^{(c)} x_1^{(c)} \right) - \left(\sum_{c=1}^k N_{,\xi}^{(c)} x_1^{(c)} \right) \left(\sum_{c=1}^k N_{,\eta}^{(c)} x_3^{(c)} \right), \quad (6c)$$

$$J_3 = \left(\sum_{c=1}^k N_{,\xi}^{(c)} x_1^{(c)} \right) \left(\sum_{c=1}^k N_{,\eta}^{(c)} x_2^{(c)} \right) - \left(\sum_{c=1}^k N_{,\xi}^{(c)} x_2^{(c)} \right) \left(\sum_{c=1}^k N_{,\eta}^{(c)} x_1^{(c)} \right). \quad (6d)$$

In Eqs.(6b)-(6d), the superscript “(c)” denotes the c -th node on the m -th element; $N_{,\xi}^{(c)}$, $N_{,\eta}^{(c)}$ represent the derivatives of the shape functions taken with respect to ξ and η , respectively. For simplification, the integrals in Eq.(5) are symbolized by

$$E_{ij}^{(c)} = \int_{-1}^1 \int_{-1}^1 N^{(c)}(\xi, \eta) U_{ij}^* |J(\xi, \eta)| d\xi d\eta, \quad (7a)$$

$$F_{ij}^{(c)} = \int_{-1}^1 \int_{-1}^1 N^{(c)}(\xi, \eta) T_{ij}^* |J(\xi, \eta)| d\xi d\eta. \quad (7b)$$

Since quadratic elements are usually employed for BEM analysis, the following derivations will be presented only for this particular case using 8 nodes for a quadrilateral element, i.e. $k=8$. Also, it should be noted that the presented formulations may be applied to a triangular element treated as a degenerate quadratic element, where three nodes of a quadrilateral side are placed at the same vertex of the triangular element. For the 8-node quadrilateral element, the shape functions take the following forms,

$$\begin{aligned} N^{(1)} &= \frac{-1}{4}(1-\xi)(1-\eta)(1+\xi+\eta), & N^{(2)} &= \frac{1}{2}(1-\xi^2)(1-\eta), \\ N^{(3)} &= \frac{1}{4}(1+\xi)(1-\eta)(\xi-\eta-1), & N^{(4)} &= \frac{1}{2}(1+\xi)(1-\eta^2), \\ N^{(5)} &= \frac{1}{4}(1+\xi)(1+\eta)(\xi+\eta-1), & N^{(6)} &= \frac{1}{2}(1-\xi^2)(1+\eta), \\ N^{(7)} &= \frac{1}{4}(1-\xi)(1+\eta)(-\xi+\eta-1), & N^{(8)} &= \frac{1}{2}(1-\xi)(1-\eta^2). \end{aligned} \quad (8)$$

Next, the processes for regularizing these integrals with different singularity orders will be elaborated separately

Integral regularization for $E_{ij}^{(c)}$

By substituting the fundamental displacements into the integrand and interpolating the coordinates using the 8-node shape functions, the integral can be expressed as

$$E_{ij}^{(c)} = \frac{1}{16\pi G(1-\nu)} \int_{-1}^1 \int_{-1}^1 \frac{N^{(c)} |J| [(3-4\nu)\delta_{ij} + r_i r_j]}{\sqrt{D(\xi, \eta)}} d\xi d\eta, \quad (9)$$

where $D(\xi, \eta)$, abbreviated simply as D , is defined by

$$D = \sum_{l=1}^3 \left(\sum_{m=1}^8 N^{(m)} x_l^{(m)} - x p_l \right)^2. \quad (10)$$

By substituting Eq.(3) into the integrand in Eq.(9), the integral can be rewritten as

$$E_{ij}^{(c)} = \frac{1}{16\pi G(1-\nu)} \left(\overline{E}_{ij}^{(c)} + \overline{\overline{E}}_{ij}^{(c)} \right), \quad (11)$$

where

$$\overline{E}_{ij}^{(c)} = (3-4\nu)\delta_{ij} \int_{-1}^1 \int_{-1}^1 \frac{N^{(c)} |J|}{\sqrt{D(\xi, \eta)}} d\xi d\eta, \quad (12a)$$

$$E_{ij}^{(c)} = \int_{-1}^1 \int_{-1}^1 \frac{N^{(c)} |J| \left(\sum_{m=1}^8 N^{(m)} x_i^{(m)} - xp_i \right) \left(\sum_{m=1}^8 N^{(m)} x_j^{(m)} - xp_j \right)}{\sqrt{D(\xi, \eta)^3}} d\xi d\eta . \quad (12b)$$

For a quadrilateral planar element depicted in Fig.1, the mid-point coordinates must satisfy

$$\begin{aligned} x_i^{(2)} &= (x_i^{(1)} + x_i^{(3)})/2, \quad x_i^{(4)} = (x_i^{(3)} + x_i^{(5)})/2, \\ x_i^{(6)} &= (x_i^{(5)} + x_i^{(7)})/2, \quad x_i^{(8)} = (x_i^{(1)} + x_i^{(7)})/2. \end{aligned} \quad (13)$$

As a direct consequence of substituting Eqs.(13) and the shape functions into Eq.(10), one obtains

$$D = \sum_{i=1}^3 A_i(\eta) \xi^2 + \sum_{i=1}^3 B_i(\eta) \xi + \sum_{i=1}^3 C_i(\eta), \quad (14)$$

where

$$A_i(\eta) = \left[\left(x_i^{(\overline{1,3})} + x_i^{(\overline{5,7})} \right) \eta - \left(x_i^{(\overline{1,3})} - x_i^{(\overline{5,7})} \right) \right]^2 / 16, \quad (15a)$$

$$\begin{aligned} B_i(\eta) &= \left((x_i^{(\overline{3,5})})^2 - (x_i^{(\overline{1,7})})^2 \right) \eta^2 / 8 + \left[x_i^{(\overline{1,3})} (x_i^{(2)} - xp_i) + x_i^{(\overline{5,7})} (x_i^{(6)} - xp_i) \right] \eta / 2 \\ &\quad - \left(x_i^{(\overline{1,3})} - x_i^{(\overline{5,7})} \right) (x_i^{(2)} + x_i^{(6)} - 2xp_i) / 4 \end{aligned} \quad (15b)$$

$$C_i(\eta) = \left[(x_i^{(2)} - x_i^{(6)}) \eta - (x_i^{(2)} + x_i^{(6)} - 2xp_i) \right]^2 / 4. \quad (15c)$$

and the $\overline{x_i^{(m,n)}}$ is defined by

$$\overline{x_i^{(m,n)}} = x_i^{(m)} - x_i^{(n)}. \quad (16)$$

In brief, Eq.(10) is rewritten as

$$D = \overline{A}(\eta) \xi^2 + \overline{B}(\eta) \xi + \overline{C}(\eta), \quad (17)$$

where

$$\overline{A}(\eta) = \sum_{i=1}^3 A_i(\eta), \quad \overline{B}(\eta) = \sum_{i=1}^3 B_i(\eta), \quad \overline{C}(\eta) = \sum_{i=1}^3 C_i(\eta). \quad (18)$$

Recall the scheme of IBP, giving

$$\int_a^b U dV = U \cdot V \Big|_a^b - \int_a^b V dU. \quad (19)$$

For applying the IBP to Eq.(12a) with respect to ξ , one may let

$$U = N^{(c)} |J|, \quad dV = \frac{d\xi}{\sqrt{\overline{A}(\eta) \xi^2 + \overline{B}(\eta) \xi + \overline{C}(\eta)}}, \quad (20)$$

and the followings are obtained,

$$dU = NJ^{(c)} d\xi, \quad V = \frac{1}{\sqrt{\overline{A}(\eta)}} \ln \left(\frac{2\overline{A}(\eta) \xi + \overline{B}(\eta)}{\sqrt{\overline{A}(\eta)}} + 2\sqrt{D(\xi, \eta)} \right), \quad (21)$$

where

$$NJ^{(c)} = \partial(N^{(c)} |J|) / \partial \xi. \quad (22)$$

Thus, operation of the IBP by Eq.(19) yields

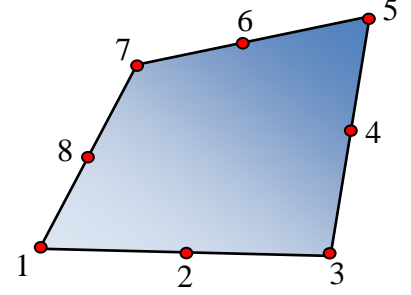


Fig.1: Nodes of a quadrilateral element

$$\int_{-1}^1 \int_{-1}^1 \frac{N^{(c)} |J|}{\sqrt{D(\xi, \eta)}} d\xi d\eta = \int_{-1}^1 G(\xi, \eta) \ln \left(\frac{2\bar{A}(\eta)\xi + \bar{B}(\eta)}{\sqrt{A(\eta)}} + 2\sqrt{D(\xi, \eta)} \right) \Big|_{\xi=-1}^{\xi=1} d\eta - \int_{-1}^1 \int_{-1}^1 F(\xi, \eta) \ln \left(\frac{2\bar{A}(\eta)\xi + \bar{B}(\eta)}{\sqrt{A(\eta)}} + 2\sqrt{D(\xi, \eta)} \right) d\xi d\eta, \quad (23)$$

where

$$G(\xi, \eta) = \frac{N^{(c)} |J|}{\sqrt{A(\eta)}}, \quad F(\xi, \eta) = \frac{NJ^{(c)}}{\sqrt{A(\eta)}}. \quad (24)$$

Still, both integrals on the right hand side of Eq.(23) reveal weak singularity that needs further regularization. For this, the single integral is expressed as

$$\int_{-1}^1 G(\xi, \eta) \ln \left(\frac{2\bar{A}(\eta)\xi + \bar{B}(\eta)}{\sqrt{A(\eta)}} + 2\sqrt{D(\xi, \eta)} \right) \Big|_{\xi=-1}^{\xi=1} d\eta = \int_{-1}^1 \left(\bar{G}(\xi', \eta) \Big|_{\xi'=1} - \bar{G}(\xi', \eta) \Big|_{\xi'=-1} \right) d\eta, \quad (25)$$

where $\bar{G}(\xi', \eta)$ is defined by

$$\bar{G}(\xi', \eta) = G(\xi', \eta) \ln \left(\frac{2\bar{A}(\eta)\xi' + \bar{B}(\eta)}{\sqrt{A(\eta)}} + 2\sqrt{D(\xi', \eta)} \right). \quad (26)$$

Firstly, the integral is rewritten as

$$\int_{-1}^1 \bar{G}(\xi', \eta) d\eta = \int_{-1}^1 \left(\bar{G}(\xi', \eta) \sqrt{\eta - \eta_0} \right) \frac{1}{\sqrt{\eta - \eta_0}} d\eta, \quad (27)$$

where η_0 is the η -coordinate of the source projection on the integration element. Numerical determination of η_0 will be elaborated later. For performing the IBP using Eq.(19), one may take

$$U = \bar{G}(\xi', \eta) \sqrt{\eta - \eta_0}, \quad dV = \frac{d\eta}{\sqrt{\eta - \eta_0}} \quad (28)$$

As a result of carrying out the IBP followed by some algebraic arrangements, one obtains

$$\int_{-1}^1 \bar{G}(\xi', \eta) d\eta = \bar{G}(\xi', \eta) (\eta - \eta_0) \Big|_{\eta=-1}^{\eta=1} - \int_{-1}^1 \bar{G}'_{\eta}(\xi', \eta) (\eta - \eta_0) d\eta, \quad (29)$$

where

$$\bar{G}'_{\eta}(\xi', \eta) = \frac{\partial \bar{G}(\xi', \eta)}{\partial \eta}. \quad (30)$$

Obviously, due to the presence of $(\eta - \eta_0)$, no more drastic fluctuation of the integrand will be present when the source point approaches the element at its projection coordinates (ξ_0, η_0) and thus, the single integral on the right hand side of Eq.(29) turns out to be regular.

Next, the effort is turned to regularize the double integral in Eq.(23). For using Eq.(19), the following substitutions are made,

$$U = F(\xi, \eta), \quad dV = \ln \left(\frac{2\bar{A}(\eta)\xi + \bar{B}(\eta)}{\sqrt{A(\eta)}} + 2\sqrt{D(\xi, \eta)} \right) d\xi. \quad (31)$$

Thus, it follows

$$dU = F'_\xi(\xi, \eta) d\xi, \quad V = \frac{2\bar{A}(\eta)\xi + \bar{B}(\eta)}{2\bar{A}(\eta)} \ln \left(\frac{2\bar{A}(\eta)\xi + \bar{B}(\eta)}{\sqrt{\bar{A}(\eta)}} + 2\sqrt{D(\xi, \eta)} \right) - \sqrt{\frac{D(\xi, \eta)}{\bar{A}(\eta)}}, \quad (32)$$

where $F'_\xi(\xi, \eta) = \partial F(\xi, \eta) / \partial \xi$. Consequentially, the use of IBP by Eq.(19) yields

$$\begin{aligned} & \int_{-1}^1 \int_{-1}^1 F(\xi, \eta) \ln \left(\frac{2\bar{A}(\eta)\xi + \bar{B}(\eta)}{\sqrt{\bar{A}(\eta)}} + 2\sqrt{D(\xi, \eta)} \right) d\xi d\eta \\ &= \int_{-1}^1 F(\xi, \eta) \left[\frac{2\bar{A}(\eta)\xi + \bar{B}(\eta)}{2\bar{A}(\eta)} \ln \left(\frac{2\bar{A}(\eta)\xi + \bar{B}(\eta)}{\sqrt{\bar{A}(\eta)}} + 2\sqrt{D(\xi, \eta)} \right) - \sqrt{\frac{D(\xi, \eta)}{\bar{A}(\eta)}} \right]_{\xi=-1}^{\xi=1} d\eta \quad (33) \\ & - \int_{-1}^1 \int_{-1}^1 F'_\xi(\xi, \eta) \left[\frac{2\bar{A}(\eta)\xi + \bar{B}(\eta)}{2\bar{A}(\eta)} \ln \left(\frac{2\bar{A}(\eta)\xi + \bar{B}(\eta)}{\sqrt{\bar{A}(\eta)}} + 2\sqrt{D(\xi, \eta)} \right) - \sqrt{\frac{D(\xi, \eta)}{\bar{A}(\eta)}} \right] d\xi d\eta \end{aligned}$$

Taking partial differentiation of $D(\xi, \eta)$ defined in Eq.(17) yields

$$\partial D(\xi, \eta) / \partial \xi = 2\bar{A}(\eta)\xi + \bar{B}(\eta). \quad (34)$$

Under the circumstance when the source point approaches the element near its projection point (ξ_0, η_0) , one will have the following conditions:

$$D(\xi_0, \eta_0) \approx 0, \quad 2\bar{A}(\eta_0)\xi_0 + \bar{B}(\eta_0) = 0. \quad (35)$$

From the above conditions, it can be seen that the double integral on the right hand side of Eq.(33) are truly regular.

For the regularization of the integral in Eq.(12b) using Eq.(19), one may take

$$U = N^{(c)} |J| \left(\sum_{m=1}^8 N^{(m)} x_i^{(m)} - xp_i \right) \left(\sum_{m=1}^8 N^{(m)} x_j^{(m)} - xp_j \right), \quad (36a)$$

$$dV = \frac{d\xi}{\sqrt{\left(\bar{A}(\eta)\xi^2 + \bar{B}(\eta)\xi + \bar{C}(\eta) \right)^3}}. \quad (36b)$$

Following the similar IBP process as before, one may obtain

$$\begin{aligned} \bar{E}_{ij}^{(c)} &= 2 \int_{-1}^1 \frac{\left[2\bar{A}(\eta)\xi' + \bar{B}(\eta) \right] H^{(c)}}{\left[4\bar{A}(\eta)\bar{C}(\eta) - \bar{B}(\eta)^2 \right] \sqrt{D(\xi', \eta)}} \Big|_{\xi'=-1}^{\xi'=1} d\eta \\ & - 2 \int_{-1}^1 \int_{-1}^1 \frac{\left[2\bar{A}(\eta)\xi + \bar{B}(\eta) \right] H'_\xi{}^{(c)}}{\left[4\bar{A}(\eta)\bar{C}(\eta) - \bar{B}(\eta)^2 \right] \sqrt{D(\xi, \eta)}} d\xi d\eta \end{aligned} \quad (37)$$

where

$$H^{(c)} = N^{(c)} |J| \left(\sum_{m=1}^8 N^{(m)} x_i^{(m)} - xp_i \right) \left(\sum_{m=1}^8 N^{(m)} x_j^{(m)} - xp_j \right), \quad H'_\xi{}^{(c)} = \frac{\partial H^{(c)}}{\partial \xi}. \quad (38)$$

It is noted that when the source point approaches the projection point (ξ_0, η_0) , one will have the following conditions,

$$H'_\xi{}^{(c)} \approx 0, \quad 2\bar{A}(\eta_0)\xi_0 + \bar{B}(\eta_0) \approx 0. \quad (39)$$

Thus, there is no spike-shape variation of the integrand of the double integral in Eq.(37). However, there is still relatively large variation of the integrands due to the presence of the term $4\bar{A}(\eta)\bar{C}(\eta) - \bar{B}(\eta)^2$ in the denominator. This can be resolved by simply sub-dividing the integral range at the projection point without resorting to further regularization processes. Up to this point,

the $E_{ij}^{(c)}$ may be numerically integrated using the regularized formulations presented above. Next, the task remains to treat the other integral by the similar IBP processes as before.

Integral regularization for $F_{ij}^{(c)}$

As aforementioned, since hyper-singularity is present for the integral $F_{ij}^{(c)}$. numerical integrations by any conventional means shall fail to yield proper values. By substituting the fundamental solution in Eq.(2b) into the integrand, the integral is written as

$$F_{ij}^{(c)} = \frac{-1}{8\pi(1-\nu)} \int_{-1}^1 \int_{-1}^1 \frac{N^{(c)}(\xi, \eta) |J(\xi, \eta)|}{r^2} \left\{ \begin{array}{l} r_{,k} n_k [(1-2\nu)\delta_{ij} + 3r_{,i} r_{,j}] \\ -(1-2\nu)(r_{,i} n_j - r_{,j} n_i) \end{array} \right\} d\xi d\eta, \quad (40)$$

where n_i , the components of the unit outward normal vector, are given by

$$n_i = \frac{J_i}{|J(\xi, \eta)|}, \quad (41)$$

and for 8-node quadrilateral planar element, J_i are calculated by

$$J_i = \varpi_{i1}\xi + \varpi_{i2}\eta + \varpi_{i3}, \quad (42)$$

where

$$\varpi_{i1} = \frac{1}{8} \left(x_{i+1}^{(5,7)} x_{i+2}^{(1,3)} - x_{i+2}^{(5,7)} x_{i+1}^{(1,3)} \right), \quad (43a)$$

$$\varpi_{i2} = \frac{1}{8} \left(x_{i+1}^{(3,5)} x_{i+2}^{(1,7)} - x_{i+2}^{(3,5)} x_{i+1}^{(1,7)} \right), \quad (43b)$$

$$\varpi_{i3} = \frac{1}{8} \left(x_{i+1}^{(1,5)} x_{i+2}^{(3,7)} - x_{i+2}^{(1,5)} x_{i+1}^{(3,7)} \right). \quad (43c)$$

In Eqs.(43a)-(43c), the subscript “ i ” follows the cyclic rule $i=(i-3)$ for $i>3$. By substituting Eq.(41) and Eq.(42) into Eq.(40), one may sort out terms to rewrite the expression as

$$F_{ij}^{(c)} = \frac{-1}{8\pi(1-\nu)} \left[(1-2\nu) \overline{F}_{ij}^{(c)} + 3 \overline{\overline{F}}_{ij}^{(c)} \right], \quad (44)$$

where

$$\overline{F}_{ij}^{(c)} = \int_{-1}^1 \int_{-1}^1 \frac{\overline{\Lambda}_{ij}^{(c)}(\xi, \eta)}{\sqrt{D^3}} d\xi d\eta, \quad (45a)$$

$$\overline{\overline{F}}_{ij}^{(c)} = \int_{-1}^1 \int_{-1}^1 \frac{\overline{\overline{\Lambda}}_{ij}^{(c)}(\xi, \eta)}{\sqrt{D^5}} d\xi d\eta, \quad (45b)$$

and $\overline{\Lambda}_{ij}^{(c)}(\xi, \eta)$, $\overline{\overline{\Lambda}}_{ij}^{(c)}(\xi, \eta)$ are given by

$$\overline{\Lambda}_{ij}^{(c)}(\xi, \eta) = N^{(c)} \delta_{ij} (X_k J_k) - X_i J_j + X_j J_i, \quad (45c)$$

$$\overline{\overline{\Lambda}}_{ij}^{(c)}(\xi, \eta) = N^{(c)} (X_k J_k) X_i X_j. \quad (45d)$$

In Eqs.(45a)-(45d), X_i is defined by

$$X_i = x_i - x p_i. \quad (46)$$

For analytically integrating the both integrals, they are re-expressed as

$$\overline{F}_{ij}^{(c)} = \int_{-1}^1 \int_{-1}^1 \frac{\sum_{m=0}^3 \Gamma_{ijm}^{(c)}(\eta) \xi^m}{\sqrt{D^3}} d\xi d\eta, \quad (47a)$$

$$\overline{\overline{F}}_{ij}^{(c)} = \int_{-1}^1 \int_{-1}^1 \frac{\sum_{m=0}^5 \Omega_{ijm}^{(c)}(\eta) \xi^m}{\sqrt{D^5}} d\xi d\eta, \quad (47b)$$

where $\Gamma_{ijm}^{(c)}$, $\Omega_{ijm}^{(c)}$ can be numerically determined by

$$\Gamma_{ijm}^{(c)}(\eta) = \frac{\left[\partial^m \overline{\Lambda}_{ij}^{(c)}(\xi, \eta) / \partial \xi^m \right]_{\xi=0}}{m!}, \quad (48a)$$

$$\Omega_{ijm}^{(c)}(\eta) = \frac{\left[\partial^m \overline{\overline{\Lambda}}_{ij}^{(c)}(\xi, \eta) / \partial \xi^m \right]_{\xi=0}}{m!}. \quad (48b)$$

In Eqs.(48a) and (48b), the partial differentiations can be performed using Eqs.(45c)-(45d) in a straightforward manner and thus, their explicit expressions are not presented here. As a result, analytical integration of Eq.(47a) with respect to ξ yields

$$\overline{F}_{ij}^{(c)} = \int_{-1}^1 \left\{ \frac{1}{\overline{A}\sqrt{D}} \left[\frac{\Psi_{ij}^{(c)}(\xi', \eta)}{\overline{A}(4\overline{AC} - \overline{B}^2)} + \Gamma_{ij3}^{(c)} \xi'^2 \right] + \frac{(2\overline{A}\Gamma_{ij2}^{(c)} - 3\overline{B}\Gamma_{ij3}^{(c)})}{2\sqrt{\overline{A}^5}} \ln \left(\frac{2\overline{A}\xi' + \overline{B}}{\sqrt{\overline{A}}} + 2\sqrt{D} \right) \right\} \Bigg|_{\xi'=-1}^{\xi'=1} d\eta, \quad (49)$$

where

$$\Psi_{ij}^{(c)}(\xi', \eta) = \begin{bmatrix} 4\overline{A}^3 \Gamma_{ij0}^{(c)} - 2\overline{A}^2 (\overline{B} \Gamma_{ij1}^{(c)} + 2\overline{C} \Gamma_{ij2}^{(c)}) \\ -3\overline{B}^3 \Gamma_{ij3}^{(c)} + 2\overline{A}\overline{B} (\overline{B} \Gamma_{ij2}^{(c)} + 5\overline{C} \Gamma_{ij3}^{(c)}) \\ + 2\overline{A}^2 (\overline{B} \Gamma_{ij0}^{(c)} - 2\overline{C} \Gamma_{ij1}^{(c)}) - 3\overline{B}^2 \overline{C} \Gamma_{ij3}^{(c)} \\ + 2\overline{A}\overline{C} (\overline{B} \Gamma_{ij2}^{(c)} + 4\overline{C} \Gamma_{ij3}^{(c)}) \end{bmatrix} \xi'. \quad (50)$$

It should be noted that near-singularity still appears in the integral in Eq.(49) due to

$$4\overline{A}(\eta_0)\overline{C}(\eta_0) - \overline{B}(\eta_0)^2 \approx 0, \quad (51)$$

and its associated integral is written as

$$\overline{f}_{ij}^{(c)} = \int_{-1}^1 \left[\frac{\Psi_{ij}^{(c)}(\xi', \eta)}{\overline{A}^2 \sqrt{D}(4\overline{AC} - \overline{B}^2)} \right] \Bigg|_{\xi'=-1}^{\xi'=1} d\eta. \quad (52)$$

From the definitions of $\overline{A}(\eta) \sim \overline{C}(\eta)$ given in Eqs.(15a)-(15c) and (18), it is clear that one may rewrite $4\overline{A}(\eta)\overline{C}(\eta) - \overline{B}(\eta)^2$, being represented by $K(\eta)$, into a quartic function of η , namely

$$K(\eta) = 4\overline{A}(\eta)\overline{C}(\eta) - \overline{B}(\eta)^2 = \sum_{m=0}^4 \alpha_m \eta^m. \quad (53)$$

Instead of explicitly sorting out all coefficients one by one, one may calculate the coefficients α_m via the fundamental calculus processes as follows:

$$\alpha_m = \frac{\left[\partial^m K(\eta) / \partial \eta^m \right]_{\eta=0}}{m!}. \quad (54)$$

For using Eq.(54), taking partial differentiation of $\bar{A}(\eta) \sim \bar{C}(\eta)$ will be involved, which can be done in a straightforward manner. From the Ferrari's method, $K(\eta)$ can be factored into a product of two quadratic polynomials, expressed as

$$K(\eta) = \alpha_4 H_1(\eta) H_2(\eta), \quad (55)$$

where

$$H_1(\eta) = (\eta^2 + \beta_1 \eta + \beta_0), \quad H_2(\eta) = (\eta^2 + \gamma_1 \eta + \gamma_0). \quad (56)$$

In Eqs.(57), the very explicit expressions for all coefficients, given in terms of α_m , can be referred to (Wikipedia online). It is worth mentioning that only one of the two functions, either $H_1(\eta)$ or $H_2(\eta)$ but not both at the same time, shall approach null for the case of near singularity. Take it as an example when

$$|H_1(\eta_0)| < \varepsilon, \quad |H_2(\eta_0)| \gg \varepsilon, \quad (57)$$

where ε is a very small value. For regularization treatment, the integral in Eq.(53) is rewritten as

$$\int_{-1}^1 \frac{\Psi_{ij}^{(c)}(\xi', \eta)}{\bar{A}^2 \sqrt{D(4\bar{A}\bar{C} - \bar{B}^2)}} d\eta = \frac{1}{\alpha_4} \int_{-1}^1 \left[\frac{\Psi_{ij}^{(c)}(\xi', \eta)}{\bar{A}^2 \sqrt{D} H_2(\eta)} \right] \frac{1}{H_1(\eta)} d\eta, \quad (58)$$

For the IBP process using Eq.(19), one may take

$$U = \left[\frac{\Psi_{ij}^{(c)}(\xi', \eta)}{\bar{A}^2 \sqrt{D} H_2(\eta)} \right], \quad dV = \frac{d\eta}{H_1(\eta)}. \quad (59)$$

As a result of performing the IBP by Eq.(19), one obtains

$$\bar{f}_{ij}^{(c)} = \frac{-2}{\alpha_4 \sqrt{\beta_1^2 - 4\beta_0}} \left\{ \begin{array}{l} \Phi_{ij}^{(c)}(\eta) \tanh^{-1} \left(\frac{2\eta + \beta_1}{\sqrt{\beta_1^2 - 4\beta_0}} \right) \Big|_{\eta=-1}^{\eta=1} \\ - \int_{-1}^1 \Phi_{ij}^{\prime(c)}(\eta) \tanh^{-1} \left(\frac{2\eta + \beta_1}{\sqrt{\beta_1^2 - 4\beta_0}} \right) d\eta \end{array} \right\}, \quad (60)$$

where

$$\Phi_{ij}^{(c)}(\eta) = \frac{\Psi_{ij}^{(c)}(\xi', \eta)}{\bar{A}^2(\eta) H_2(\eta) \sqrt{D(\xi', \eta)}} \Big|_{\xi'=-1}^{\xi'=1}, \quad \Phi_{ij}^{\prime(c)}(\eta) = \frac{\partial \Phi_{ij}^{(c)}(\eta)}{\partial \eta}. \quad (61)$$

Eventually, the integral $\bar{F}_{ij}^{(c)}$ is thus given by

$$\bar{F}_{ij}^{(c)} = \bar{f}_{ij}^{(c)} + \int_{-1}^1 \left[\frac{\Gamma_{ij3}^{(c)} \xi'^2}{\bar{A} \sqrt{D}} + \frac{(2\bar{A} \Gamma_{ij2}^{(c)} - 3\bar{B} \Gamma_{ij3}^{(c)})}{2\sqrt{\bar{A}^5}} \ln \left(\frac{2\bar{A} \xi' + \bar{B}}{\sqrt{\bar{A}}} + 2\sqrt{D} \right) \right]_{\xi'=-1}^{\xi'=1} d\eta. \quad (62)$$

Next, the similar regularization treatment can be carried out for $\bar{F}_{ij}^{(c)}$, given in Eq.(47b). Analytical integration of the integral with respect to ξ leads to

$$\bar{F}_{ij}^{(c)} = \bar{f}_{ij}^{(c)} + \int_{-1}^1 \left[\frac{\Omega_{ij5}^{(c)} \xi'^4}{\bar{A} \sqrt{D}^3} + \frac{(2\bar{A} \Omega_{ij4}^{(c)} - 5\bar{B} \Omega_{ij5}^{(c)})}{2\sqrt{\bar{A}^7}} \ln \left(\frac{2\bar{A} \xi' + \bar{B}}{2\sqrt{\bar{A}}} + \sqrt{D(\xi', \eta)} \right) \right]_{\xi'=-1}^{\xi'=1} d\eta, \quad (63)$$

where

$$\overline{f}_{ij}^{(c)} = \int_{-1}^1 \frac{\sum_{k=0}^3 \Upsilon_{ijk}^{(c)} \xi^k / \sqrt{D^3}}{3A^3 (4\overline{AC} - \overline{B}^2)^2} \Big|_{\xi^t=-1}^{\xi^t=1} d\eta, \quad (64)$$

and the $\Upsilon_{ijk}^{(c)}$ is defined as follows:

$$\begin{aligned} \Upsilon_{ij3}^{(c)} = & 4\Omega_{ij5}^{(c)} \overline{AB} \left(5\overline{B}^4 + 64\overline{A}^2 \overline{C}^2 - 37\overline{AC} \overline{B}^2 \right) - 16\Omega_{ij1}^{(c)} \overline{A}^5 \overline{B} \\ & - 8\Omega_{ij4}^{(c)} \overline{A}^2 \left(8\overline{A}^2 \overline{C}^2 + \overline{B}^4 - 7\overline{AC} \overline{B}^2 \right) + 32\Omega_{ij0}^{(c)} \overline{A}^6, \end{aligned} \quad (65a)$$

$$\begin{aligned} & - 2\Omega_{ij3}^{(c)} \overline{A}^3 \overline{B} \left(12\overline{AC} - \overline{B}^2 \right) + 4\Omega_{ij2}^{(c)} \overline{A}^4 \left(4\overline{AC} + \overline{B}^2 \right) \\ \Upsilon_{ij2}^{(c)} = & 3\Omega_{ij5}^{(c)} \left(16\overline{A}^2 \overline{B}^2 \overline{C}^2 + 64\overline{A}^3 \overline{C}^3 - 30\overline{B}^4 \overline{AC} + 5\overline{B}^6 \right) \\ & + \left(6\Omega_{ij2}^{(c)} \overline{A}^3 \overline{B} - 12\Omega_{ij3}^{(c)} \overline{CA} \right) \left(4\overline{AC} + \overline{B}^2 \right), \end{aligned} \quad (65b)$$

$$\begin{aligned} \Upsilon_{ij1}^{(c)} = & 6\Omega_{ij5}^{(c)} \overline{BC} \left(5\overline{B}^4 - 35\overline{AC} \overline{B}^2 + 52\overline{A}^2 \overline{C}^2 \right) - 48\Omega_{ij3}^{(c)} \overline{A}^3 \overline{BC}^2 \\ & + 12\Omega_{ij4}^{(c)} \overline{AC} \left(7\overline{AC} \overline{B}^2 - 4\overline{A}^2 \overline{C}^2 - \overline{B}^4 \right) + 24\Omega_{ij2}^{(c)} \overline{A}^3 \overline{B}^2 \overline{C}, \end{aligned} \quad (65c)$$

$$\begin{aligned} \Upsilon_{ij0}^{(c)} = & \Omega_{ij5}^{(c)} \overline{C}^2 \left(15\overline{B}^4 - 100\overline{AC} \overline{B}^2 + 128\overline{A}^2 \overline{C}^2 \right) + 16\Omega_{ij2}^{(c)} \overline{A}^3 \overline{C}^2 \overline{B} \\ & + 2\Omega_{ij4}^{(c)} \overline{ABC}^2 \left(20\overline{AC} - 3\overline{B}^2 \right) - 32\Omega_{ij3}^{(c)} \overline{A}^3 \overline{C}^3 \\ & - 4\Omega_{ij1}^{(c)} \overline{A}^3 \overline{C} \left(4\overline{AC} + \overline{B}^2 \right) + 2\Omega_{ij0}^{(c)} \overline{A}^3 \overline{B} \left(12\overline{AC} - \overline{B}^2 \right) \end{aligned} \quad (65d)$$

Likewise, the integral in Eq.(64) still reveals near singularity under the condition as described in Eq.(51). For this, the integral is rewritten as

$$\overline{f}_{ij}^{(c)} = \frac{1}{3\alpha_4^2} \int_{-1}^1 \frac{\Lambda(\eta)}{H_2(\eta)^2} \frac{1}{H_1(\eta)^2} d\eta, \quad (66)$$

where $\Lambda(\eta)$ is defined by

$$\Lambda(\eta) = \frac{\sum_{k=0}^3 \Upsilon_{ijk}^{(c)} \xi^k / \sqrt{D^3}}{A^3} \Big|_{\xi^t=-1}^{\xi^t=1}. \quad (67)$$

For applying the IBP onto Eq.(66), one may let

$$U = \frac{\Lambda(\eta)}{H_2(\eta)^2}, \quad dV = \frac{d\eta}{H_1(\eta)^2}, \quad (68)$$

and thus, the use of Eq.(19) yields

$$f_{ij}^{(c)} = \frac{1}{3\alpha_4^2} \left(\frac{\Lambda(\eta')}{H_2(\eta')^2} \left[\frac{4}{\sqrt{(4\beta_0 - \beta_1^2)^3}} \tan^{-1} \left(\frac{\beta_1 + 2\eta'}{\sqrt{4\beta_0 - \beta_1^2}} \right) + \frac{\beta_1 + 2\eta'}{H_1(\eta')(4\beta_0 - \beta_1^2)} \right] \right)_{\eta'=-1}^{\eta'=1} - \int_{-1}^1 Z(\eta) d\eta, \quad (69)$$

where $Z(\eta)$ is defined by

$$Z(\eta) = \frac{\partial(\Lambda(\eta)/H_2(\eta)^2)}{\partial\eta} \left\{ \frac{4}{\sqrt{(4\beta_0 - \beta_1^2)^3}} \tan^{-1} \left(\frac{\beta_1 + 2\eta}{\sqrt{4\beta_0 - \beta_1^2}} \right) + \frac{\beta_1 + 2\eta}{H_1(\eta)(4\beta_0 - \beta_1^2)} \right\}. \quad (70)$$

Due to the following condition

$$\beta_1 + 2\eta_0 \approx 0, \quad (71)$$

the integrand defined in Eq.(70) is indeed regular when the source point approaches the element under integration. In the sequel, the resulting regularized integral can be calculated by Eq.(63) and Eq.(69). However, it should be noted that although the regularized forms may now be integrated by any conventional numerical schemes, relative higher integration order is still needed for yielding satisfactorily accurate results. This is mainly because the certain fluctuations of the integrands still remain, although not so drastic like the un-regularized forms. Nevertheless, the cost of greater integration order is minor since the integrations are performed only for single-integrals. Also, a good practice for improving the accuracy is to subdivide the integration element into 4 quadrants at the project point (ξ_0, η_0) . At this point, discussion about how to numerically determine the projection coordinates is elaborated next.

Determination of the projection point

As explained earlier, under the nearly singular condition when the source point approaches the integration element, the integrand will become drastically large at its projection coordinates (ξ_0, η_0) . It is clear that when the source point approaches the element near (ξ_0, η_0) , the denominator of the integrand will be verging to null. Evidently, the numerical value of $D(\xi_0, \eta_0)$ should be the minimum, leading to the following conditions:

$$D'_\xi(\xi_0, \eta_0) = \left. \frac{\partial D(\xi, \eta)}{\partial \xi} \right|_{\substack{\xi=\xi_0 \\ \eta=\eta_0}} = 0, \quad D'_\eta(\xi_0, \eta_0) = \left. \frac{\partial D(\xi, \eta)}{\partial \eta} \right|_{\substack{\xi=\xi_0 \\ \eta=\eta_0}} = 0. \quad (72)$$

For performing the partial differentiations described above, Eq.(17) is reformulated into the following form:

$$D(\xi, \eta) = \hat{A}(\xi)\eta^2 + \hat{B}(\xi)\eta + \hat{C}(\eta), \quad (73)$$

where

$$\hat{A}(\xi) = \frac{1}{16} \sum_{i=1}^3 \left[\left(\hat{x}_i^{(1,7)} - \hat{x}_i^{(3,5)} \right) \xi - \left(\hat{x}_i^{(1,7)} + \hat{x}_i^{(3,5)} \right) \right]^2, \quad (74a)$$

$$\begin{aligned} \hat{B}(\xi) &= \sum_{i=1}^3 \left(\left\langle \hat{x}_i^{(5,7)} \right\rangle^2 - \left\langle \hat{x}_i^{(1,3)} \right\rangle^2 \right) \frac{\xi^2}{8} \\ &+ \sum_{i=1}^3 \left[\hat{x}_i^{(1,7)} (\hat{x}_i^{(8)} - \hat{x}_{p_i}) - \hat{x}_i^{(3,5)} (\hat{x}_i^{(4)} - \hat{x}_{p_i}) \right] \frac{\xi}{2}, \quad (74b) \\ &- \frac{1}{4} \sum_{i=1}^3 \left(\hat{x}_i^{(1,7)} + \hat{x}_i^{(3,5)} \right) (\hat{x}_i^{(2)} + \hat{x}_i^{(6)} - 2\hat{x}_{p_i}) \end{aligned}$$

$$\hat{C}(\eta) = \frac{1}{4} \sum_{i=1}^3 \left[(\hat{x}_i^{(8)} - \hat{x}_i^{(4)}) \xi - (\hat{x}_i^{(8)} + \hat{x}_i^{(4)} - 2\hat{x}_i) \right]^2. \quad (74c)$$

Obviously, analytically solving the two simultaneous equations in Eqs.(72) is absolutely not an easy task. Alternatively, they can be numerically solved in an iterative manner. Firstly, one may adopt $\xi_1=0$ as the initial shooting point and then, by use of Eqs.(72), perform the following repetitive iterations to yield a convergent solution:

$$\eta_i = \frac{-\hat{B}(\xi_i)}{2\hat{A}(\xi_i)}, \quad \xi_{i+1} = \frac{-\bar{B}(\eta_i)}{2\bar{A}(\eta_i)}, \quad (75)$$

where the subscript “ i ” is used to denote the i -th iteration time. From the iterative process, fast convergence is assured to give the projection coordinates (ξ_0, η_0) .

Although the fully regularized integrals presented above are ideal substitutes for the original, their numerical evaluations shall cost more CPU-runtime as a tradeoff. For this reason, the computer code should be programmed in such a way that it can discriminate the special condition when the regularized integrals are supposed to be invoked. This can be easily achieved by use of the following criteria:

$$|D(\xi_0, \eta_0) / D_{ave}| \leq \varepsilon, \quad (76)$$

where ε is a small value chosen by the user and D_{ave} is the average value of $D(\xi, \eta)$ for all element nodes. That is, under the regular condition, the integrals are evaluated in a conventional manner as usual; the regularized ones are used as the substitutes only when the criteria, Eq.(76), is met. In what follows, numerical examples will be studied for testing the accuracy of the regularized integrals.

Numerical examples

For verifying the validity of the proposed formulations, consider a typical case assuming $\nu=0.3$, Young’s modulus=1000 (units) and an element with the following arbitrarily chosen nodal coordinates:

$$\begin{aligned} x_1^{(1)} &= -30, & x_2^{(1)} &= -50, & x_3^{(1)} &= 1, \\ x_1^{(3)} &= 50, & x_2^{(3)} &= -60, & x_3^{(3)} &= 1, \\ x_1^{(5)} &= 70, & x_2^{(5)} &= 30, & x_3^{(5)} &= 1, \\ x_1^{(7)} &= -40, & x_2^{(7)} &= 40, & x_3^{(7)} &= 1, \\ xp_1 &= 2, & xp_2 &= 1, & xp_3 &= 1 - \delta, \end{aligned} \quad (77)$$

where δ is a small distance away from the element. For this test case, the average dimensional length of all four edges, denoted by L , is about 93.456371. By the iteration process as described earlier, a convergent solution $(\xi_0 \approx -0.2248131, \eta_0 \approx 0.219465)$ was obtained for the projection coordinates.

Displayed in Table 1 are the computed values of $E_{11}^{(c)}$, serving to be a typical example of $E_{ij}^{(c)}$. Since all other components of $E_{ij}^{(c)}$ have similar computation accuracy, they are not presented here. For providing a comparison base, the software MathCAD, employing the scheme of adaptive integration, was used to perform the numerical integrations. For the conventional numerical integrations, 14-point Gauss integrations of the both original and the regularized forms were carried out. Since the MathCAD has convergence difficulty for $\delta \approx 10^{-3}$, the distance δ ranging from 10^0 to 10^{-2} was used for the test, resulting the δ/L as low as 10^{-4} that is sufficiently small for most practical

applications. Also, as a typical example of $F_{ij}^{(c)}$, the numerical results of the computed $F_{11}^{(c)}$ are tabulated in Table 2. As can be observed from these tables, with the decreasing δ , Gauss integrations of the original forms will be getting off accuracy as compared with the MathCAD results, while the accuracies of the regularized integrations are satisfactory.

Table 1: Computed $E_{11}^{(c)}$ for decreasing δ

δ (δL)		10^0 ($\approx 1.7E-2$)	10^{-1} ($\approx 1.7E-3$)	10^{-2} ($\approx 1.7E-4$)
c	$ D(\xi_0, \eta_0)/D_{ave} $	2.8614E-4	2.8623E-6	2.8623E-8
1	MathCAD	-7.4115E-3	-7.6819E-3	-7.7095E-3
	Original (% Diff.)	-7.0456E-3 (4.94%)	-7.0861E-3 (7.76%)	-7.0865E-3 (8.08%)
	Regularized (% Diff.)	-7.4109E-3 (0.01%)	-7.6924E-3 (0.14%)	-7.7036E-3 (0.08%)
2	MathCAD	1.6877E-2	1.7302E-2	1.7345E-2
	Original (% Diff.)	1.6311E-2 (3.36%)	1.6377E-2 (5.35%)	1.6377E-2 (5.58%)
	Regularized (% Diff.)	1.6877E-2 (0.00%)	1.7312E-2 (0.06%)	1.7326E-2 (0.11%)
3	MathCAD	-7.3512E-3	-7.6003E-3	-7.6257E-3
	Original (% Diff.)	-7.0161E-3 (4.56%)	-7.0540E-3 (7.19%)	-7.0544E-3 (7.49%)
	Regularized (% Diff.)	-7.3509E-3 (0.00%)	-7.6061E-3 (0.08%)	-7.6147E-3 (0.14%)
4	MathCAD	1.8390E-2	1.8814E-2	1.8857E-2
	Original (% Diff.)	1.7823E-2 (3.08%)	1.7890E-2 (4.91%)	1.7891E-2 (5.12%)
	Regularized (% Diff.)	1.8390E-2 (0.00%)	1.8824E-2 (0.05%)	1.8839E-2 (0.10%)
5	MathCAD	-6.9679E-3	-7.2379E-3	-7.2655E-3
	Original (% Diff.)	-6.6035E-3 (5.23%)	-6.6438E-3 (8.21%)	-6.6442E-3 (8.55%)
	Regularized (% Diff.)	-6.9676E-3 (0.00%)	-7.2442E-3 (0.09%)	-7.2535E-3 (0.17%)
6	MathCAD	2.3228E-2	2.3891E-2	2.3958E-2
	Original (% Diff.)	2.2348E-2 (3.79%)	2.2452E-2 (6.02%)	2.2453E-2 (6.28%)
	Regularized (% Diff.)	2.3227E-2 (0.00%)	2.3906E-2 (0.06%)	2.3929E-2 (0.12%)
7	MathCAD	-6.2830E-3	-6.5184E-3	-6.5425E-3
	Original (% Diff.)	-5.9644E-3 (5.07%)	-5.9992E-3 (7.96%)	-5.9996E-3 (8.30%)
	Regularized (% Diff.)	-6.2832E-3 (0.00%)	-6.5173E-3 (0.02%)	-6.5225E-3 (0.31%)
8	MathCAD	2.2970E-2	2.3639E-2	2.3707E-2
	Original (% Diff.)	2.2074E-2 (3.90%)	2.2179E-2 (6.17%)	2.2180E-2 (6.44%)
	Regularized (% Diff.)	2.2967E-2 (0.02%)	2.3701E-2 (0.26%)	2.3744E-2 (0.16%)

Table 2: Computed $F_{11}^{(c)}$ for decreasing δ

δ (δL)		10^0 ($\approx 1.7E-2$)	10^{-1} ($\approx 1.7E-3$)	10^{-2} ($\approx 1.7E-4$)
c	$ D(\xi_0, \eta_0)/D_{ave} $	2.8614E-4	2.8623E-6	2.8623E-8
1	MathCAD	1.1214E-1	1.1818E-1	1.1879E-1
	Original (% Diff.)	3.6264E-2 (67.66%)	3.7705E-3 (96.81%)	3.7720E-4 (99.68%)
	Regularized (% Diff.)	1.1214E-1 (0.00%)	1.1810E-1 (0.07%)	1.2255E-1 (3.16%)
2	MathCAD	-1.7664E-1	-1.8440E-1	-1.8518E-1
	Original (% Diff.)	-5.8502E-2 (66.88%)	-6.0774E-3 (96.70%)	-6.0798E-4 (99.67%)
	Regularized (% Diff.)	-1.7664E-1 (0.00%)	-1.8426E-1 (0.08%)	-1.9103E-1 (3.16%)
3	MathCAD	1.0353E-1	1.0865E-1	1.0918E-1
	Original (% Diff.)	3.3860E-2 (67.29%)	3.5192E-3 (96.76%)	3.5206E-4 (99.68%)
	Regularized (% Diff.)	1.0353E-1 (0.00%)	1.0858E-1 (0.07%)	1.1263E-1 (3.16%)
4	MathCAD	-1.7810E-1	-1.8382E-1	-1.8440E-1
	Original (% Diff.)	-6.0295E-2 (66.14%)	-6.2557E-3 (96.60%)	-6.2580E-4 (99.66%)
	Regularized (% Diff.)	-1.7810E-1 (0.00%)	-1.8370E-1 (0.06%)	-1.9022E-1 (3.16%)
5	MathCAD	1.1154E-1	1.1806E-1	1.1870E-1
	Original (% Diff.)	3.5812E-2 (67.89%)	3.7251E-3 (96.84%)	3.7266E-4 (99.69%)
	Regularized (% Diff.)	1.1154E-1 (0.00%)	1.1798E-1 (0.07%)	1.2247E-1 (3.18%)
6	MathCAD	-2.7619E-1	-2.8812E-1	-2.8932E-1
	Original (% Diff.)	-9.2103E-2 (66.65%)	-9.5682E-3 (96.68%)	-9.5719E-4 (99.67%)
	Regularized (% Diff.)	-2.7619E-1 (0.00%)	-2.8795E-1 (0.06%)	-2.9847E-1 (3.16%)
7	MathCAD	9.7323E-2	1.0309E-1	1.0369E-1
	Original (% Diff.)	3.1168E-2 (67.98%)	3.2417E-3 (96.86%)	3.2429E-4 (99.69%)
	Regularized (% Diff.)	9.7323E-2 (0.00%)	1.0302E-1 (0.07%)	1.0696E-1 (3.16%)
8	MathCAD	-2.7985E-1	-2.9028E-1	-2.9134E-1
	Original (% Diff.)	9.3671E-2 (66.53%)	-9.7299E-3 (96.65%)	-9.7337E-4 (99.67%)
	Regularized (% Diff.)	-2.7985E-1 (0.02%)	-2.9009E-1 (0.07%)	-3.0054E-1 (3.16%)

For demonstrating the successful implementation in an existing BEM code, the second example considers a clamped-clamped thin plate subjected to uniform pressure as depicted in Fig.2. Also shown in this figure is the BEM discretization that employs 28 quadratic elements. Simply for the purpose of verification, the problem is fully modeled to check the symmetry of data output. For the material properties, $E=1000$ (units) and $\nu=0.3$ are used. The thickness ratio D/L is chosen to be 0.1 and 0.01 as two typical cases, testing the accuracy of our BEM analysis. Providing a comparison base, finite element analyses by ANSYS were also carried out. Figures 3(a) and 3(b) show the plots of the calculated transverse displacement (u_3/P) along the centerline $x_1=0$ for $D/L=0.1$ and 0.01, respectively. As can be seen from these plots, for $D/L=0.1$, the both BEM approaches- the conventional and the regularization scheme provide consistent results as compared with the ANSYS analysis. However, for the D/L falling to 0.01, the conventional BEM approach fails to yield consistent results, while the present approach still gives ideal results in agreement with the ANSYS analysis.

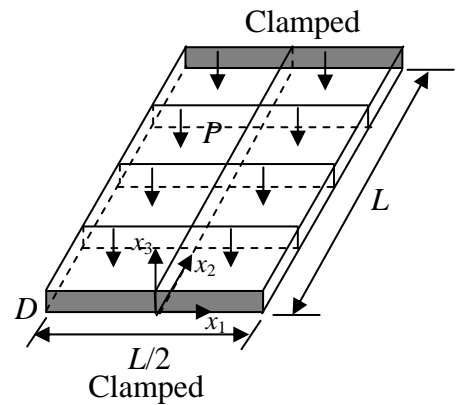


Fig.2: A clamped-clamped thin plate subjected to uniform pressure on top

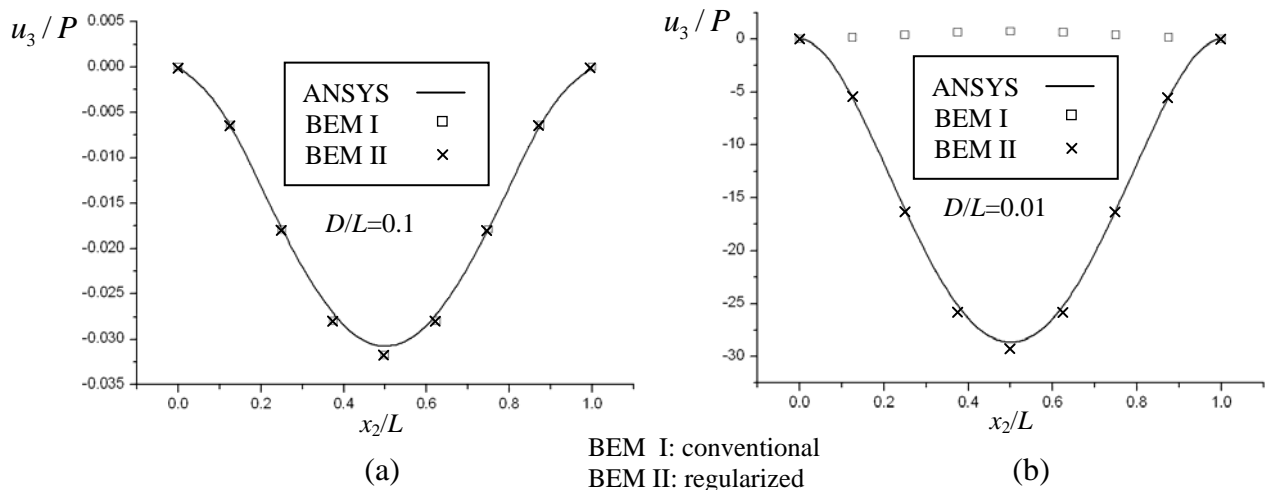


Fig.3: Normalized transverse displacement along the centerline of the thin plate for (a) $D/L=0.1$ and (b) $D/L=0.01$

Conclusive remarks

For analyzing the elastic field of thin bodies or at interior points near the boundary, integrations of the boundary integrals will have the numerical difficulty of so called "near singularity". This paper presents a regularization scheme, applying the approach of integration by parts, to regularize the strongly singular and hyper singular integrals for the elastostatic BEM analysis. In the past, this scheme has only been used for 2D problems; the present work is to demonstrate its extension to treat 3D elastostatic analysis. In this paper, only planar elements are treated, for which the associated integrals are integrated by parts to formulate regularized forms. As a typical example for the demonstration, derivations for quadrilateral elements are presented; nevertheless, the similar processes can be applied to a triangular element, treated as a degenerated quadrilateral element with three nodes of one side coincided at the same vertex. For verifying the validity of the regularized integrals, numerical tests were experimented for a typical example. The results show that the

regularized integral can be numerically integrated by the Gauss Quadrature scheme, although slightly more Gauss points are needed to guarantee satisfactory accuracy. The proposed regularization treatments have not been implemented to 3D BEM code yet. Further research is required for studying the accuracy of the BEM implementation and its computational efficiency.

Acknowledgement

The authors gratefully acknowledge the financial support for this work from the National Science Council of Taiwan (NSC 99-2221-E-006-259-MY3).

References

- Chen, J.T. and Hong, H-K. (1999), Review of dual boundary element methods with emphasis on hypersingular integrals and divergent series. *Applied Mechanics Reviews*, 52(1), pp.17-33.
- Granados, J.J. and Gallego, R. (2001), Regularization of nearly hypersingular integrals in the boundary element method, *Engineering Analysis with Boundary Elements*, 25 (3), pp. 165-184.
- Guz, A.N. and Zozulya, V.V. (2001), Fracture dynamics with allowance for a crack edges contact interaction, *International Journal of Nonlinear Sciences and Numerical Simulation*, 2(3), pp. 173-233.
- Lacerda, L.A. de and Wrobel, L.C., (2001), Hypersingular boundary integral equation for axisymmetric elasticity, *Int. J. Numer. Meth. Engng*, 52, pp.1337-1354.
- Reddy, J.N. (1984), *Energy and Variational Methods in Applied Mechanics: With an Introduction to the Finite Element Method*, John Wiley & Sons, p.346.
- Shiah, Y.C. and Shi, Yi-Xiao (2006), Heat conduction across thermal barrier coatings of anisotropic substrates, *International Communications in Heat and Mass Transfer*, 33 (7), pp.827-835.
- Shiah, Y.C., Chen, Y.H., and W.S. Kuo (2007), Analysis for the Interlaminar Stresses of Thin Layered Composites subjected to Thermal Loads, *Composites Science and Technology*, 67, pp.2485-2492.
- Tanaka, M., Sladek, V., and Sladek, J. (1994), Regularization techniques applied to boundary element methods. *Applied Mechanics Reviews*, 47(10), pp.457-499.
- Tomioka, Satoshi and Nishiyama, Shusuke (2010), Analytical regularization of hypersingular integral for Helmholtz equation in boundary element method, *Engineering Analysis with Boundary Elements*, 34 (4), pp. 393-404.
- Wikipedia online, https://en.wikipedia.org/wiki/Quartic_function.
- Zozulya, V.V. (2010), Divergent Integrals in Elastostatics: Regularization in 3-D Case, *CMES: Computer Modeling in Engineering & Sciences*, 70(3), 253-349.